

Laterally Mobile, Functionalized Self-Assembled Monolayers at the Fluorous–Aqueous Interface in a Plug-Based Microfluidic System: Characterization and Testing with Membrane Protein Crystallization

Jason E. Kreutz, Liang Li, L. Spencer Roach, Takuji Hatakeyama, and Rustem F. Ismagilov*

Department of Chemistry, The University of Chicago, 929 East 57th Street, Chicago, Illinois 60637

Received November 8, 2008; Revised Manuscript Received March 26, 2009; E-mail: r-ismagilov@uchicago.edu

This paper describes a method to generate functionalizable, mobile self-assembled monolayers (SAMs) in plug-based microfluidics. Control of interfaces is advancing studies of biological interfaces, heterogeneous reactions, and nanotechnology. SAMs have been useful for such studies,^{1,2} but SAMs are not laterally mobile² and so are less applicable to systems where motion along the interface is important, such as protein crystallization,^{3–5} or when multiple membrane-associated proteins must assemble to perform their function.⁶ Lipid-based methods such as monolayers, vesicles, black lipid membranes, and supported lipid bilayers are typically mobile but less robust and less stable than SAMs. Lipid-based methods effectively form 2-D crystals of proteins, but successes⁵ with nucleation of 3-D crystals are rare, presumably because salts, PEG, and detergents used in crystallization experiments perturb lipid structures. Although these methods are widely used, increasing their throughput capacity remains a work in progress.⁷

Plug-based microfluidics⁸ can generate thousands of unique reaction mixtures as droplets surrounded by a fluorocarbon, allowing for rapid and expansive exploration of chemical space.^{9–11} We previously developed a fluorosurfactant with an oligoethylene glycol head-group,¹² designated RfOEG, that assembles at the fluorous–aqueous interface and prevents nonspecific adsorption of proteins. A variation of this approach has been described.¹³ Here we implemented his-tag binding chemistry to design RfNTA, which introduces specific adsorption of proteins at the interface (Figure 1a), and we showed that this system offers interfacial functionality and mobility. We then applied this approach to the crystallization of a 6-histidine-tagged membrane protein, reaction center (hRC), performed 2400 crystallization trials, and showed that it can increase the range of successful conditions, the success rate at a given condition, the rate of nucleation, and the quality of the crystals formed.

To synthesize RfNTA we attached a nitrilotriacetate (NTA) head-group to RfOEG (Scheme S1). In the Supporting Information we report an improved one-step synthesis of RfOEG with ~30% yield under Mitsunobu conditions.¹⁴ We used a his-tagged green fluorescent protein (hGFP) to demonstrate that a complex of RfNTA with Ni²⁺ (RfNTA: Ni) introduced specific interactions with his-tagged proteins at the plug interface. Alone, hGFP was uniformly distributed in the plug (Figure 1b, e); with RfNTA: Ni, the hGFP was concentrated at the interface (Figure 1c, f). Other surfactants were added to test whether they interfere with the specific interaction introduced by RfNTA: Ni. The presence of RfOEG did not interfere (Figure 1d, g), as supported by surface tension measurements (Figure S1). Furthermore, all hGFP experiments contained 0.05% w/v lauryldimethylamine *N*-oxide (LDAO), showing that hydrocarbon detergents that solubilize membrane proteins did not interfere with the system.

Control experiments showed that interfacial adsorption was dependent on the formation of the RfNTA: Ni:hGFP complex. When adding (a) only Ni²⁺, (b) only RfNTA, or (c) a complex of Ni²⁺ and NTA, with no fluorosurfactant, to hGFP (Figure S2a–c), the fluorescence

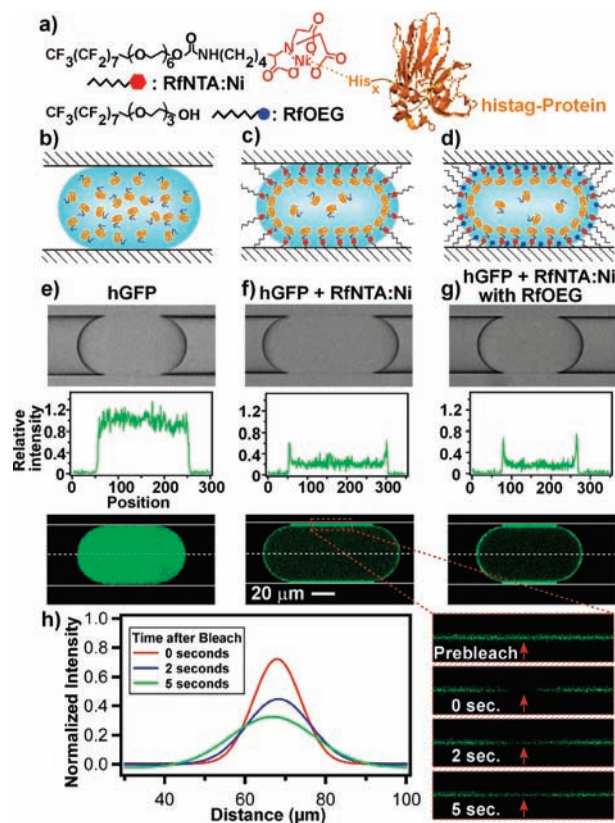


Figure 1. His-tagged GFP (hGFP) and a 10-histidine peptide labeled with fluorescein (His10) were used to visualize the interfacial adsorption and mobility of the RfNTA: Ni:hProtein complex. (a) Structure of RfNTA: Ni (top) and RfOEG (bottom). (b–d) Schematics of assembly of proteins when (b) only the protein is present, (c) the RfNTA: Ni:hProtein complex forms and (d) when RfOEG is also present. (e–g) Brightfield images (top), fluorescent images (bottom), and line scans along the long axis of the plug (middle) for plugs containing 400 nM hGFP with (e) no additive, (f) 12 μ M RfNTA: Ni added, and (g) 25 μ M RfNTA: Ni with RfOEG at 860 μ M in FC-40. All plugs contained 100 mM Tris pH 7.0 and 0.05% w/v lauryldimethylamine *N*-oxide (LDAO). (h) Gaussian fits across the bleach spot over time (left) and corresponding fluorescence images over the course of an FRAP experiment (right). The images in (h) were from the region of plug represented by the box in (f). His10 at 3.7 μ M, 30 μ M RfNTA: Ni in 20 mM Tris pH 8.0, and 170 μ M RfOEG in FC-70 were used in (h).

was uniform across the plug. Addition of EDTA (12 mM) (Figure S2d) and imidazole (120 mM) (data not shown) disrupted interfacial adsorption.

Fluorescence recovery after photobleaching (FRAP) experiments showed that the functionalized interface remained mobile (Figures 1h, S3, S4, S5, and Table S1). A 10-histidine peptide labeled with fluorescein (His10), which can bind multiple RfNTA: Ni molecules,¹⁵ was used to exclude the possibility that rebinding kinetics was measured instead of interfacial diffusion. The profiles of the bleach

spots were fit to Gaussian curves to obtain diffusion coefficients¹⁶ for His10 of $(7.3 \pm 2.6) \times 10^{-12}$, $(15.2 \pm 2.4) \times 10^{-12}$, and $(39.2 \pm 11.5) \times 10^{-12}$ m²/s for FC-70 (viscosity of 12 cSt at RT), FC-40 (1.8 cSt), and FC-84 (0.53 cSt), respectively (Figure S4 and Table S1), which are comparable to those of lipids or lipid anchored proteins in monolayers and bilayers, including proteins anchored by NTA:Ni $((1-50) \times 10^{-12}$ m²/s).¹⁷ The dependence of recovery on the viscosity of the fluorocarbon strongly supports interfacial diffusion as a mechanism of recovery of fluorescence. hGFP gave comparable results, but quenching between the molecules at the interface¹⁸ prevented quantitative analysis (Figure S5).

Binding of proteins to RfNTA:Ni at the interface results in increased local supersaturation and a decrease in degrees of freedom, reducing the entropy cost, which lowers the energy barriers to nucleation. Thus, RfNTA:Ni should aid membrane protein crystallization in the following ways: (1) Increase the range of successful conditions for crystallization. (2) Increase the success rate of protein crystallization under a given condition. (3) Improve the quality of crystals. Higher quality crystals could result from slower growth at lower precipitant concentrations. RfNTA:Ni should be compatible with a wider range of crystallization conditions than lipid-based analogues because, like other fluorinated molecules containing NTA,⁴ it resists interference by detergents.

To test these hypotheses, we used hRC from *Rhodobacter sphaeroides* (Figure 2).¹⁹ When RfNTA:Ni was added, nucleation occurred more quickly (Figure 2b), crystals formed in more trials, (Figures 2a, S6, and S7), and diffraction quality was typically higher (Table S2 and Figure S8) than that under standard conditions. With only Ni²⁺ added, all nucleation was suppressed, indicating that Ni²⁺ inhibits crystal formation (Figure 2b). With only RfNTA added, results were similar to those under standard conditions, but nucleation was faster (Figure 2a, b), possibly due to a residual amount of divalent cations leaching into solution from the microfluidic device.²⁰ At high concentrations of RfNTA:Ni and at the highest concentration of precipitant, the number of crystals actually decreased, due either to interference from nonspecific adsorption through surface histidines or to nucleation occurring too rapidly for ordered growth. When 10 mM imidazole was added, the rate of crystal formation and the number and quality of crystals were restored (Figure 2 and Table S2). These results were reproducible for another preparation of the protein, but the generality of this approach to many proteins remains to be tested.

This paper demonstrates a method complementary to current SAM and lipid methods for rapid generation of mobile, functionalized SAMs

that are compatible with easily exploring large areas of chemical space, both in solution and at interfaces. Here we explored the chemical space of the solution phase, but surface composition in this system can also be varied by changing the tagging functionalities of surfactants at the interface or by varying the tagged molecules in solution. Such variations will allow application of this method to other processes, such as nucleation of protein aggregates,²¹ multicomponent interfacial assembly, and capture assays that rely on binding to the interface and do not require washing steps.²² The use of additional analytical techniques compatible with plugs, such as in situ diffraction,¹⁰ mass spectrometry,⁹ fluorescence correlation spectroscopy,²³ and chemistries would further expand the method's applicability.

Acknowledgment. This work was funded in part by ATCG3D U54 GM074961 and by the NIH T32 GM008720 (J.E.K.). We thank Phil Laible of Argonne National Laboratory for the generous gift of hRC, Vytautas Bindokas Matthias Meier and Mikhail Karymov for help with FRAP experiments and data processing, and Elizabeth B. Haney for contributions in editing and writing this manuscript.

Supporting Information Available: Detailed procedure for synthesis and experiments and additional figures. This material is available free of charge via the Internet at <http://pubs.acs.org>.

References

- Gurard-Levin, Z. A.; Mrksich, M. *Annu. Rev. Anal. Chem.* **2008**, *1*, 767–800.
- Love, J. C.; Estroff, L. A.; Kriebel, J. K.; Nuzzo, R. G.; Whitesides, G. M. *Chem. Rev.* **2005**, *105*, 1103–1169.
- Courty, S.; Lebeau, L.; Martel, L.; Lenne, P. F.; Balavoine, F.; Dischert, W.; Kononov, O.; Mioskowski, C.; Legrand, J. F.; Venien-Bryan, C. *Langmuir* **2002**, *18*, 9502–9512.
- Dauvergne, J.; Polidori, A.; Venien-Bryan, C.; Pucci, B. *Tetrahedron Lett.* **2008**, *49*, 2247–2250.
- Darst, S. A.; Edwards, A. M. *Curr. Opin. Struct. Biol.* **1995**, *5*, 640–644.
- Gureasko, J.; Galush, W. J.; Boykevich, S.; Sondermann, H.; Bar-Sagi, D.; Groves, J. T.; Kuriyan, J. *Nat. Struct. Mol. Biol.* **2008**, *15*, 452–461.
- (a) Groves, J. T.; Boxer, S. G. *Acc. Chem. Res.* **2002**, *35*, 149–157. (b) Shi, J.; Yang, T.; Cremer, P. S. *Anal. Chem.* **2008**, *80*, 6078–6084.
- (a) Song, H.; Chen, D. L.; Ismagilov, R. F. *Angew. Chem., Int. Ed.* **2006**, *45*, 7336–7356. (b) Song, H.; Tice, J. D.; Ismagilov, R. F. *Angew. Chem., Int. Ed.* **2003**, *42*, 768–772.
- Hatakeyama, T.; Chen, D. L.; Ismagilov, R. F. *J. Am. Chem. Soc.* **2006**, *128*, 2518–2519.
- Li, L.; Mustafi, D.; Fu, Q.; Tereshko, V.; Chen, D. L.; Tice, J. D.; Ismagilov, R. F. *Proc. Natl. Acad. Sci. U.S.A.* **2006**, *103*, 19243–19248.
- (a) Laval, P.; Lisai, N.; Salmon, J. B.; Joanicot, M. *Lab Chip* **2007**, *7*, 829–834. (b) Shim, J. U.; Cristobal, G.; Link, D. R.; Thorsen, T.; Jia, Y. W.; Piattelli, K.; Fraden, S. *J. Am. Chem. Soc.* **2007**, *129*, 8825–8835. (c) Lau, B. T. C.; Baitz, C. A.; Dong, X. P.; Hansen, C. L. *J. Am. Chem. Soc.* **2007**, *129*, 454–455.
- Roach, L. S.; Song, H.; Ismagilov, R. F. *Anal. Chem.* **2005**, *77*, 785–796.
- Holtz, C.; Rowat, A. C.; Agresti, J. J.; Hutchison, J. B.; Angile, F. E.; Schmitz, C. H. J.; Koster, S.; Duan, H.; Humphry, K. J.; Scanga, R. A.; Johnson, J. S.; Pisignano, D.; Weitz, D. A. *Lab Chip* **2008**, *8*, 1632–1639.
- Falck, J. R.; Yu, J.; Cho, H.-S. *Tetrahedron Lett.* **1994**, *35*, 5997–6000.
- Nye, J. A.; Groves, J. T. *Langmuir* **2008**, *24*, 4145–4149.
- Seiffert, S.; Oppermann, W. *J. Microsc.-Oxf.* **2005**, *220*, 20–30.
- (a) Schubert, T.; Barmann, M.; Rusp, M.; Granzer, W.; Tanaka, M. *J. Membr. Sci.* **2008**, *321*, 61–68. (b) Adalsteinsson, T.; Yu, H. *Langmuir* **2000**, *16*, 9410–9413. (c) Tanaka, M.; Hermann, J.; Haase, L.; Fischer, M.; Boxer, S. G. *Langmuir* **2007**, *23*, 5638–5644.
- Robeson, J. L.; Tilton, R. D. *Biophys. J.* **1995**, *68*, 2145–2155.
- Allen, J. P.; Feher, G.; Yeates, T. O.; Rees, D. C.; Deisenhofer, J.; Michel, H.; Huber, R. *Proc. Natl. Acad. Sci. U.S.A.* **1986**, *83*, 8589–8593.
- Kothe, M.; Kohls, D.; Low, S.; Coli, R.; Cheng, A. C.; Jacques, S. L.; Johnson, T. L.; Lewis, C.; Loh, C.; Nonomiyama, J.; Sheils, A. L.; Verdries, K. A.; Wynn, T. A.; Kuhn, C.; Ding, Y. H. *Biochemistry* **2007**, *46*, 5960–5971.
- Meier, M.; Kennedy-Darling, J.; Choi, S. H.; Norstrom, E. M.; Sisodia, S. S.; Ismagilov, R. F. *Angew. Chem., Int. Ed.* **2009**, *48*, 1487–1489.
- Einav, S.; Gerber, D.; Bryson, P. D.; Sklan, E. H.; Elazar, M.; Maerkl, S. J.; Glenn, J. S.; Quake, S. R. *Nat. Biotechnol.* **2008**, *26*, 1019–1027.
- Chen, D. L.; Du, W. B.; Liu, Y.; Liu, W. S.; Kuznetsov, A.; Philipson, L. H.; Ismagilov, R. F. *Proc. Natl. Acad. Sci. U.S.A.* **2008**, *105*, 16843–16848.

JA808697E

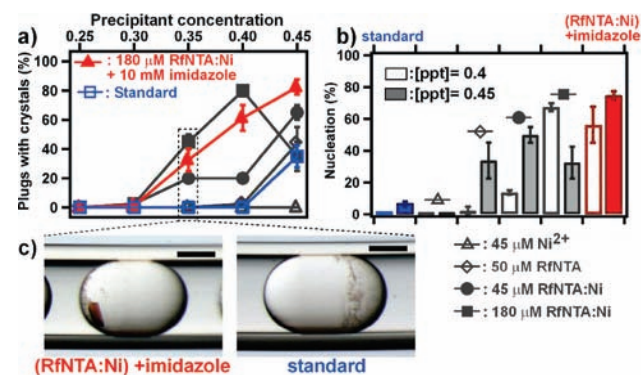


Figure 2. Interfacial adsorption of his-tagged reaction center (hRC) enhances crystal nucleation. (a) The addition of RfNTA:Ni resulted in a greater range of successful conditions. (b) The relative rate of nucleation increased upon addition of RfNTA:Ni. The graph shows the two highest concentrations of precipitant for different additives. (c) Microphotographs of plugs for standard conditions (right) and conditions containing 200 μ M RfNTA:Ni with 10 mM imidazole (left). Scale bar is 100 μ m.